Supplemental Information for "Mechanical genomics identifies diverse modulators of bacterial cell-stiffness"

George K. Auer[1], Timothy K. Lee[2,^], Manohary Rajendram[3,^], Spencer Cesar[4], Amanda Miguel[2], Kerwyn Casey Huang[2,4,*], and Douglas B. Weibel[1,3,5,*]

1. Department of Biomedical Engineering, University of Wisconsin-Madison, Madison, WI 53706, USA

2. Department of Bioengineering, Stanford University, Stanford, CA 94305, USA

3. Department of Biochemistry, University of Wisconsin-Madison, Madison, WI 53706, USA

4. Department of Microbiology and Immunology, Stanford University School of Medicine, Stanford, CA 94305, USA

5. Department of Chemistry, University of Wisconsin-Madison, Madison, WI 53706, USA

[^]Equal contributions

[*]To whom correspondence should be addressed: weibel@biochem.wisc.edu and kchuang@stanford.edu

SUPPLEMENTAL FIGURES

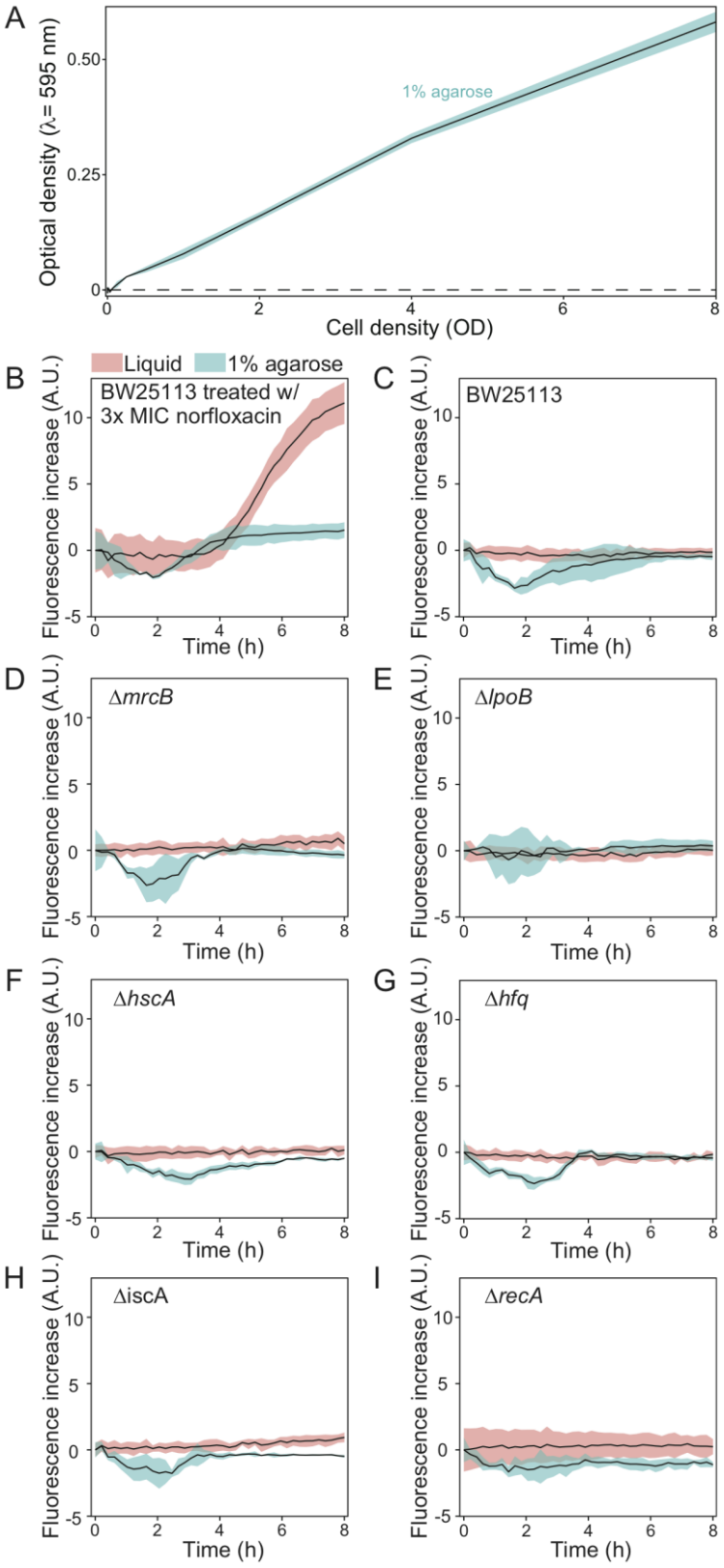

Figure S1: Measurement of optical density and SOS response of *E. coli* cells embedded in 1% agarose, related to Figure 1.

(A) Optical density of *E. coli* BW25113 cells embedded in 1% agarose exhibits an approximately linear increase with increasing cell density. Shaded region represents one standard deviation above and below mean growth curve (n = 3 curves).

(B) When *E. coli* BW25113 cells were treated with norfloxacin at three times the minimum inhibitory concentration (MIC), we observed induction of the SOS response in both liquid and agarose. Cells with a *sulA* promoter fusion to GFP were grown in wells of a 96-well plate and fluorescence (λ_{ex} = 485 nm, λ_{em} = 515 nm) was quantified using a plate reader. To normalize fluorescence signal to cell density, the optical density was monitored at λ = 595 nm. Shaded regions represent one standard deviation above and below mean growth curves (n = 3 biological replicates). A.U., arbitrary units.

(C-I) SOS induction was negligible in both liquid and agarose for wild-type cells and six mutants with large-magnitude GRABS scores. Optical density and fluorescence was monitored as in (B).

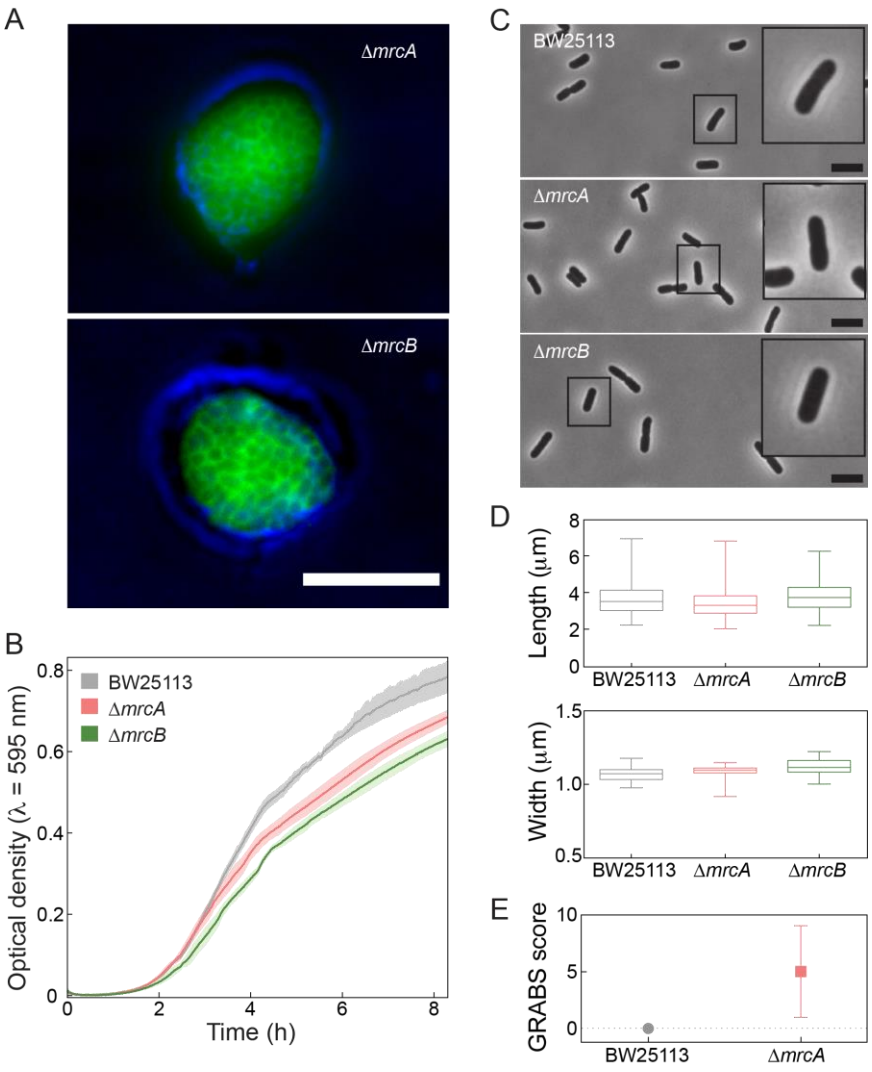

Figure S2: Δ*mrcA* and Δ*mrcB* cells have distinct mechanical properties, yet their growth rates in liquid and cell morphology in liquid and agarose are similar to each other, related to Figure 2.

A) Δ*mrcA* and Δ*mrcB* cells do not exhibit substantial changes in cell size or shape after 8 h of growth embedded in 1% agarose. Blue is a false color of the phase-contrast image. Green is a false color of the fluorescence channel from FM4-64 membrane stain. Scale bar: 10 μm.

B) Δ*mrcA* and Δ*mrcB* cells have similar growth rates, with slight growth-rate deficiencies relative to wild-type, in liquid LB. Growth curves were measured by monitoring optical absorbance. Solid lines represent the mean over $n = 3$ curves. Shaded regions represent one standard deviation away from the mean. Maximum growth rates, obtained by fitting to a Gompertz relation: (BW25113, 0.01 min^{-1}; Δ*mrcA*, 0.0072 min^{-1}; Δ*mrcB*, 0.0077 min^{-1}).

C) Phase-contrast images of *E. coli* BW25113, Δ*mrcA*, and Δ*mrcB* cells grown in liquid LB. Scale bar: 5 μm.

D) Δ*mrcA* and Δ*mrcB* cells have similar cellular dimensions as wild-type cells ($n \geq 217$ cells for each strain). Error bars represent one standard deviation from the mean.

E) Δ*mrcA* cells have a GRABS score indicating that their stiffness is similar to wild-type cells. By definition, wild-type cells have a GRABS score of zero because all measurements are normalized to the wells containing wild-type cells. Error bars are one standard deviation away from the mean ($n = 4$).

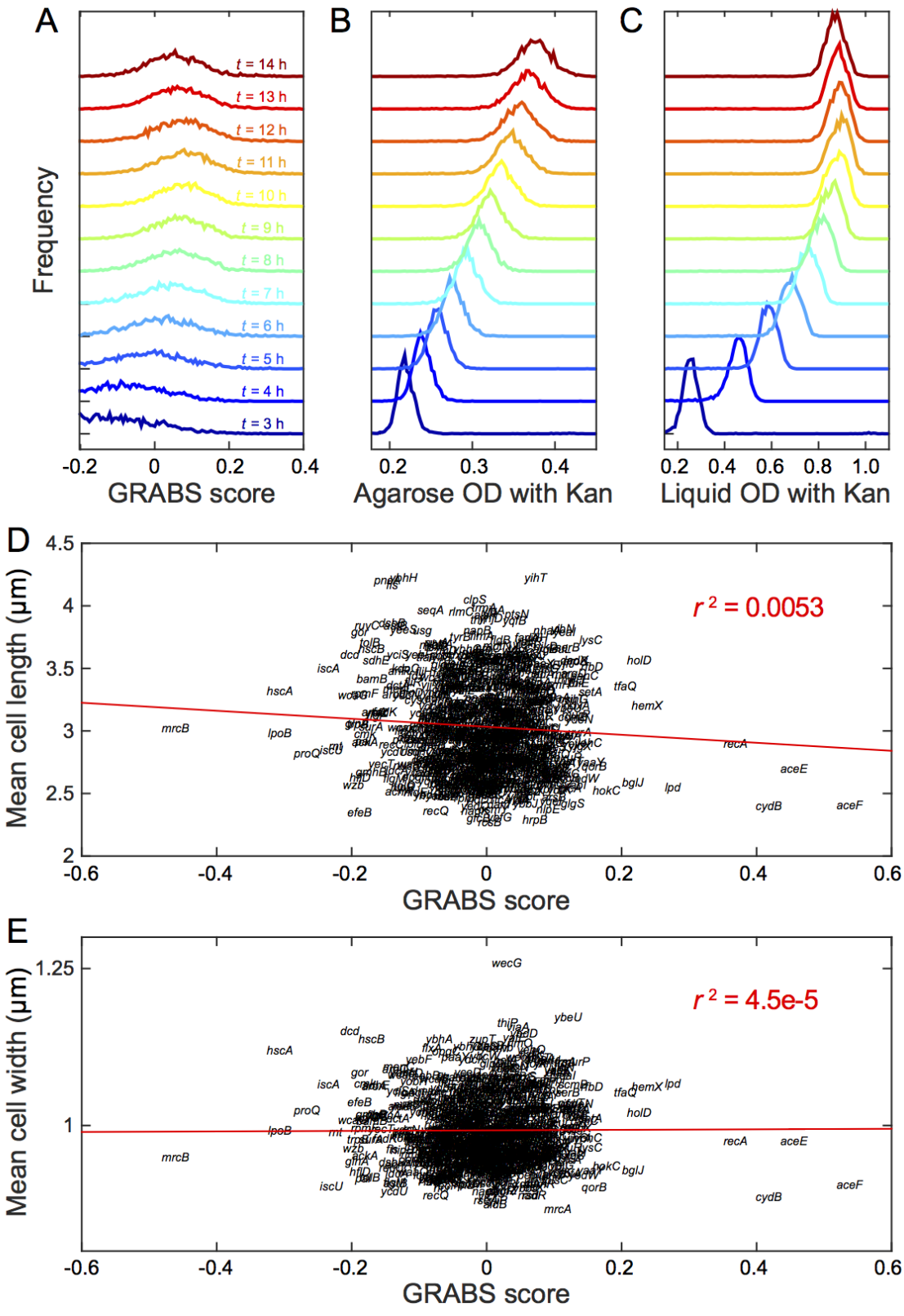
A
B
C
Frequency
t = 14 h
t = 13 h
t = 12 h
t = 11 h
t = 10 h
t = 9 h
t = 8 h
t = 7 h
t = 6 h
t = 5 h
t = 4 h
t = 3 h
-0.2 0 0.2 0.4
GRABS score
0.2 0.3 0.4
Agarose OD with Kan
0.2 0.4 0.6 0.8 1.0
Liquid OD with Kan
D
Mean cell length (μm)
4.5
4
3.5
3
2.5
2
r 2 = 0.0053
-0.6 -0.4 -0.2 0 0.2 0.4 0.6
GRABS score
E
Mean cell width (μm)
1.25
1
r 2 = 4.5e-5
-0.6 -0.4 -0.2 0 0.2 0.4 0.6
GRABS score

Figure S3: Distributions of GRABS scores over time for all Keio strains and their correlation to cellular dimensions, related to Figure 2.

(A) Distribution of GRABS scores over time. GRABS scores were calculated as described in the Extended Experimental Procedures, but with the time point of the final OD measurement varied from t = 3 h to t = 14 h. Curves are shown with variable shifts along the y-axis for visual clarity. The largest range of GRABS scores occurred after ~8 h of growth.

(B) Distribution of OD values for agarose-embedded growth over time. Kan, kanamycin.

(C) Distribution of OD values for liquid growth over time. Kan, kanamycin.

(D) GRABS scores are not significantly correlated with average cell width, $n \geq$ 100 cells for each strain. (Extended Experimental Methods; p = 0.075)

(E) GRABS scores are not significantly correlated with average cell length, $n \geq$ 100 cells for each strain. (Extended Experimental Methods; p = 0.68)

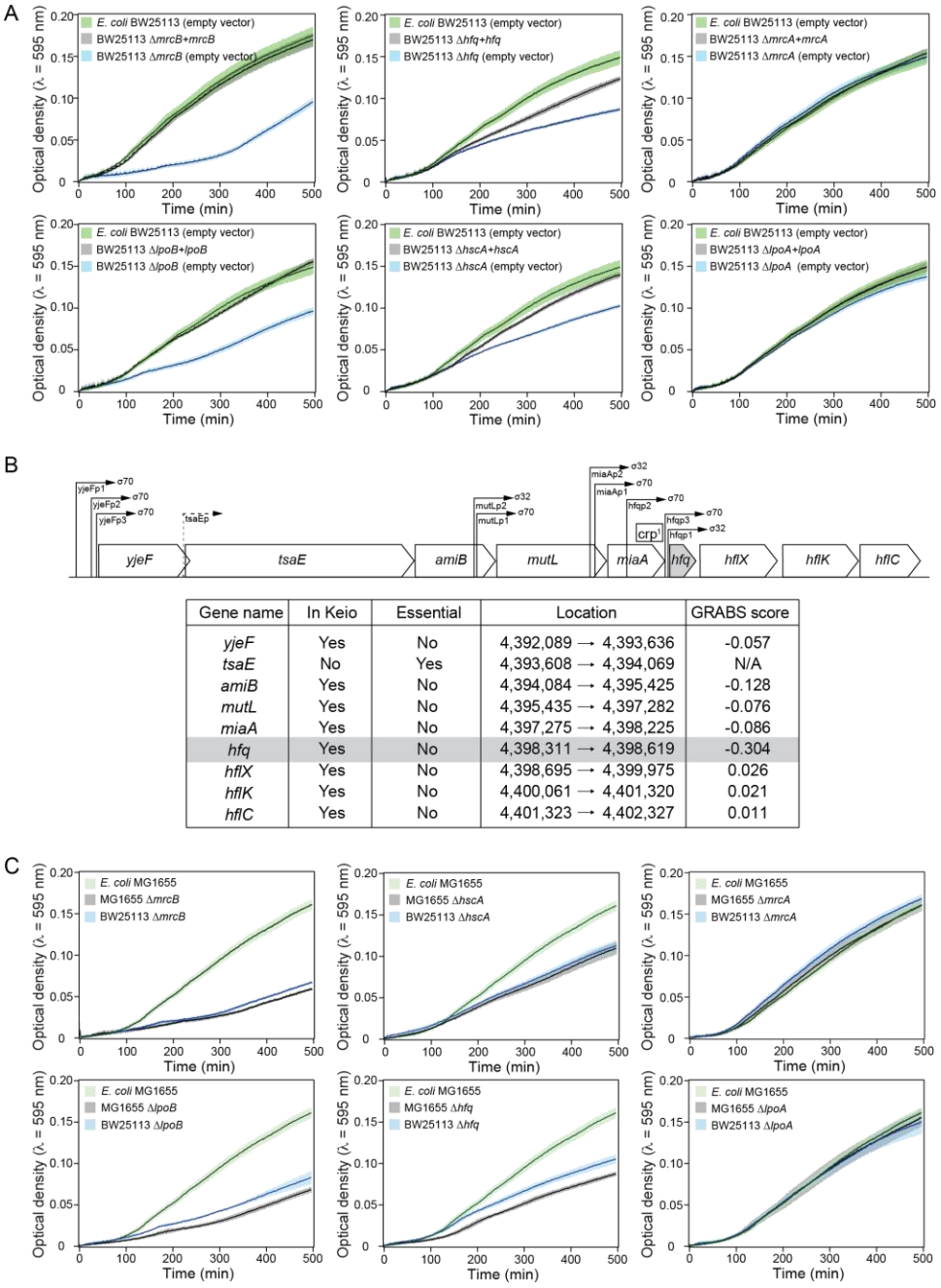

Gene name	In Keio	Essential	Location	GRABS score
yjeF	Yes	No	4,392,089 → 4,393,636	-0.057
tsaE	No	Yes	4,393,608 → 4,394,069	N/A
amiB	Yes	No	4,394,084 → 4,395,425	-0.128
mutL	Yes	No	4,395,435 → 4,397,282	-0.076
miaA	Yes	No	4,397,275 → 4,398,225	-0.086
hfq	Yes	No	4,398,311 → 4,398,619	-0.304
hflX	Yes	No	4,398,695 → 4,399,975	0.026
hflK	Yes	No	4,400,061 → 4,401,320	0.021
hflC	Yes	No	4,401,323 → 4,402,327	0.011

Figure S4: Clean deletions in *E. coli* MG1655 and complementation studies validate GRABS measurements of Keio strains, related to Figure 2.

A) Complementation of four genes that yielded large decreases in GRABS score (*mrcB*, *lpoB*, *hfq*, and *hscA*) and two genes that produced

essentially no stiffness change (*mrcA* and *lpoA*) resulted in recovery of mechanical defects when the cells were embedded in 1% agarose. Average growth curves (solid lines) of agarose-embedded *E. coli* BW25113 cells with an empty vector (green) compared to growth curves of Keio BW25113 mutants complemented in *trans* indicate 80-100% recovery after 8 h in Δ*mrcB*, Δ*lpoB*, Δ*hfq*, and Δ*hscA* and no change in Δ*mrcA* and Δ*lpoA*. Shaded regions represent one standard deviation above and below mean growth curves (n = 6).

B) We detected no mechanical phenotypes in deletions of genes downstream of *hfq* in the operon containing *hfq*. *tsaE* is not included in the Keio collection and therefore we did not test it.

C) The phenotypes of *E. coli* MG1655 mutants embedded in agarose are quantitatively similar to those of the corresponding BW25113 mutants after 8 h. Mean agarose-embedded growth curves of *E. coli* MG1655 (green) and selected gene deletions in MG1655 (black) and BW25113 (blue). Shaded regions represent one standard deviation above and below the mean (n = 6).

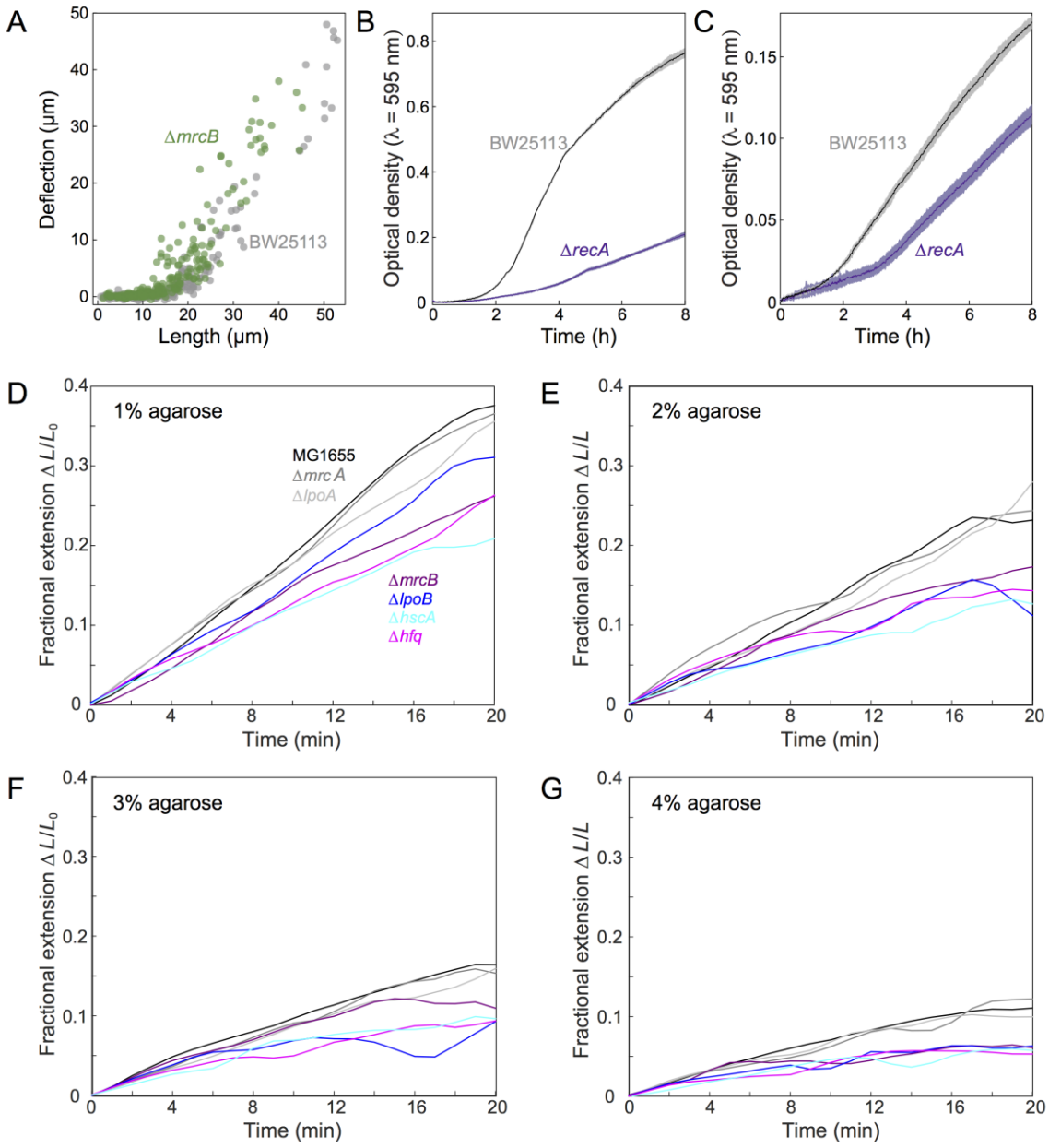

103

104 **Figure S5: Responses of *E. coli* mutants to external force, related to Figure 3**

105 **and Figure 4.**

106 (A)Deflection of cells in microfluidic bending device. Greater deflection of

107 Δ*mrcB* cells relative to wild-type cells of the same length indicates a

decrease in cell stiffness. Circles represent deflection values along the flow direction for individual cells (n > 200 cells, two independent experiments).

(B) Δ*recA* cells exhibit much slower growth in liquid than wild-type BW25113 cells. Solid lines are means of n = 3 growth curves; shaded regions represent one standard deviation about the mean.

(C) Δ*recA* cells exhibit similar growth in agarose as wild-type BW25113 cells. Solid lines are means of n = 3 growth curves; shaded regions represent one standard deviation about the mean.

(D-G) Single-cell, microscopy-based measurements of elongation inhibition agree with GRABS data. Average fractional elongation curves while embedded in 1-4% agarose gels for wild-type and six deletion strains of *E. coli* MG1655. The Δ*mrcB*, Δ*lpoB*, Δ*hfq*, Δ*hscA* mutants consistently display increased inhibition of elongation compared to wild-type, Δ*mrcA*, and Δ*lpoA* cells, as predicted by GRABS scores. L_0, initial cell length; ΔL, the change in length relative to t = 0. Curves are averages over single-cell trajectories and were smoothed over a 5-min window. The number of cells measured decreases over the course of the experiment as some cell trajectories become difficult to track; the initial number of trajectories for a given mutant and agarose concentration ranged from 26-79 across experiments.

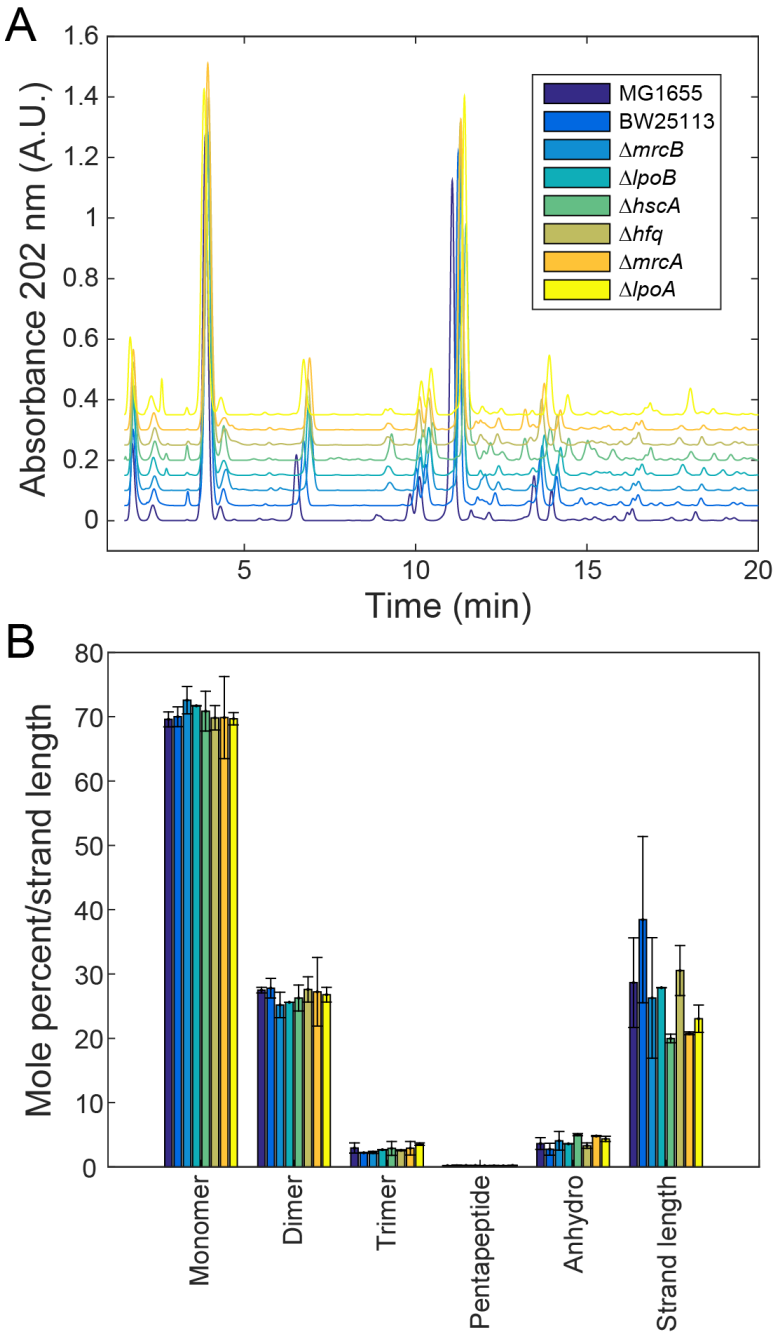

Figure S6: UPLC analysis of mutants shows no striking differences in peptidoglycan composition between wildtype and several mutants with most negative GRABS scores, related to Figure 3.

(A) Chromatograms of purified cell walls from *E. coli* MG1655, BW25113, and six Keio mutants, including four with large, negative GRABS scores (Δ*mrcB*, Δ*hscA*, Δ*lpoB*, and Δ*hfq*) and two with GRABS scores close to zero (Δ*mrcA* and Δ*lpoA*). Cell walls were purified and digested, and samples were analyzed using UPLC (Extended Experimental Procedures). Chromatograms were normalized to have the same integrated total absorbance and overlaid with baselines staggered for easier comparison. No substantial differences among the chromatograms were evident.

(B) Molar fractions of monomers, dimers, trimers, pentapeptides, and anhydro peaks, as well as the glycan strand length computed from total anhydro fraction, were quantified. The low abundance of anhydro species typically leads to greater variability in the calculation of average strand length.

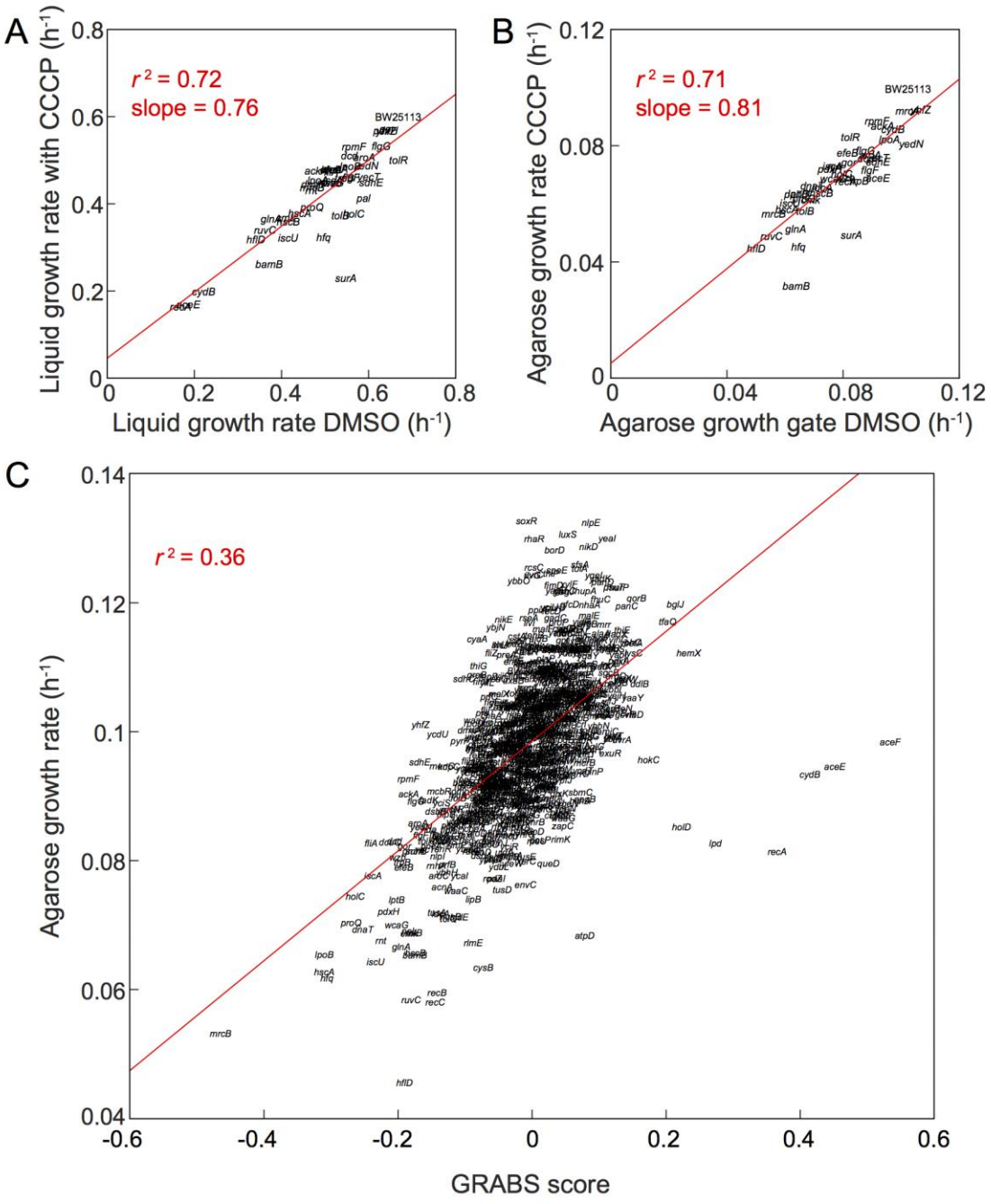

145

146 **Figure S7: Carbonyl cyanide *m*-chlorophenyl hydrazone (CCCP) generally**

147 **reduces growth rates and the relation of the GRABS score to maximal growth**

148 **rates in agarose, related to Figure 5 and Figure 2.**

(A) Fractional growth-rate of Keio mutants treated with CCCP in liquid. DMSO, dimethyl sulfoxide..

(B) Fractional growth-rate of Keio mutants treated with CCCP in agarose is reduced compared to liquid as evidenced by the difference in slopes. DMSO, dimethyl sulfoxide.

(C) GRABS scores are correlated with maximal growth rates in agarose. Growth rates were obtained by fitting growth curves for encapsulated cells with a Gompertz relation. The highly significant correlation ($p < 10^{-81}$) indicates that agarose growth rate is a reasonable proxy for GRABS score, potentially simplifying experimental design and analysis, although this simplification is less accurate for some mutants.

SUPPLEMENTAL TABLES

Table S1. Gene Ontology (GO) enrichment of GRABS hits, related to Figure 2 and Figure 3.

GO Term	Counts	Definition
GO:0016226	3	iron-sulfur cluster assembly
GO:0009242	2	colanic acid biosynthetic process
GO:0043165	2	Gram-negative-bacterium-type cell outer membrane assembly
GO:0006457	3	protein folding
GO:0043213	2	bacteriocin transport
GO:0006260	3	DNA replication
GO:0015949	2	nucleobase-containing small molecule interconversion
GO:0000162	1	tryptophan biosynthetic process
GO:0006082	1	organic acid metabolic process
GO:0006083	1	acetate metabolic process
GO:0006085	1	acetyl-CoA biosynthetic process
GO:0006105	1	succinate metabolic process
GO:0006220	1	pyrimidine nucleotide metabolic process
GO:0006226	1	dUMP biosynthetic process
GO:0006229	1	dUTP biosynthetic process
GO:0006267	1	pre-replicative complex assembly involved in nuclear cell cycle DNA replication
GO:0006542	1	glutamine biosynthetic process
GO:0006568	1	tryptophan metabolic process
GO:0006749	1	glutathione metabolic process
GO:0007059	1	chromosome segregation
GO:0009220	1	pyrimidine ribonucleotide biosynthetic process
GO:0009399	1	nitrogen fixation
GO:0009443	1	pyridoxal 5'-phosphate salvage
GO:0010608	1	posttranscriptional regulation of gene expression
GO:0015740	1	C4-dicarboxylate transport
GO:0017013	1	protein flavinylation
GO:0019395	1	fatty acid oxidation

GO:0019413	1	acetate biosynthetic process
GO:0019542	1	propionate biosynthetic process
GO:0019676	1	ammonia assimilation cycle
GO:0032298	1	positive regulation of DNA-dependent DNA replication initiation
GO:0033212	1	iron assimilation
GO:0040033	1	negative regulation of translation, ncRNA-mediated
GO:0042351	1	'de novo' GDP-L-fucose biosynthetic process
GO:0042780	1	tRNA 3'-end processing
GO:0042816	1	vitamin B6 metabolic process
GO:0044092	1	negative regulation of molecular function
GO:0045975	1	positive regulation of translation, ncRNA-mediated
GO:0046080	1	dUTP metabolic process
GO:0051050	1	positive regulation of transport
GO:0051085	1	chaperone mediated protein folding requiring cofactor
GO:0051259	1	protein oligomerization
GO:0060274	1	maintenance of stationary phase
GO:0071932	1	replication fork reversal
GO:0009073	2	aromatic amino acid family biosynthetic process
GO:0009252	2	peptidoglycan biosynthetic process
GO:0000271	1	polysaccharide biosynthetic process
GO:0000725	1	recombinational repair
GO:0006259	1	DNA metabolic process
GO:0006269	1	DNA replication, synthesis of RNA primer
GO:0008156	1	negative regulation of DNA replication
GO:0015684	1	ferrous iron transport
GO:0015920	1	lipopolysaccharide transport
GO:0019740	1	nitrogen utilization
GO:0032297	1	negative regulation of DNA-dependent DNA replication initiation
GO:0044237	1	cellular metabolic process
GO:0050821	1	protein stabilization
GO:0051205	1	protein insertion into membrane
GO:0070417	1	cellular response to cold
GO:0097171	1	ADP-L-glycero-beta-D-manno-heptose biosynthetic process
GO:0008360	2	regulation of cell shape

GO:0042710	2	biofilm formation
GO:0015031	2	protein transport
GO:0001123	1	transcription initiation from bacterial-type RNA polymerase promoter
GO:0006261	1	DNA-dependent DNA replication
GO:0006807	1	nitrogen compound metabolic process
GO:0009117	1	nucleotide metabolic process
GO:0017038	1	protein import
GO:0044781	1	bacterial-type flagellum organization
GO:0071973	2	bacterial-type flagellum-dependent cell motility
GO:0006352	1	DNA-templated transcription, initiation
GO:0008615	1	pyridoxine biosynthetic process
GO:0006631	1	fatty acid metabolic process
GO:0010468	1	regulation of gene expression
GO:0006396	1	RNA processing
GO:0006928	1	movement of cell or subcellular component
GO:0045454	1	cell redox homeostasis
GO:0009423	1	chorismate biosynthetic process
GO:0006629	1	lipid metabolic process
GO:0009244	1	lipopolysaccharide core region biosynthetic process
GO:0008033	1	tRNA processing
GO:0006508	1	proteolysis
GO:0006310	1	DNA recombination
GO:0006412	1	translation
GO:0009408	1	response to heat
GO:0008652	2	cellular amino acid biosynthetic process
GO:0046677	1	response to antibiotic
GO:0016310	2	phosphorylation
GO:0006281	1	DNA repair
GO:0009103	1	lipopolysaccharide biosynthetic process
GO:0006974	3	cellular response to DNA damage stimulus
GO:0005975	1	carbohydrate metabolic process
GO:0008152	3	metabolic process
GO:0055114	4	oxidation-reduction process
GO:0006355	2	regulation of transcription, DNA-templated
GO:0006810	4	transport
GO:0006351	1	transcription, DNA-templated

Table S2. Clusters of Orthologous Groups (COGs) for GRABS hits, related to Figure 2 and Figure 3.

COG code	Counts	Definition
A	1	RNA processing and modification
C	8	Energy production and conversion
E	4	Amino acid transport and metabolism
F	2	Nucleotide transport and metabolism
G	1	Carbohydrate transport and metabolism
H	1	Coenzyme transport and metabolism
J	1	Translation, ribosomal structure, and biogenesis
K	2	Transcription
L	6	Replication, recombination, and repair
M	9	Cell wall, membrane, and envelope biogenesis
N	3	Cell motility
O	3	Posttranslational modification and metabolism
P	1	Inorganic ion transport and metabolism
R	1	General function prediction only
S	3	Function unknown
T	3	Signal transduction mechanisms
U	3	Intracellular trafficking, secretion, and vesicular transport
V	1	Cytoskeleton

Table S3: Chemical-genomics conditions with the largest-magnitude positive Pearson correlation coefficients with stiffness scores. Related to Figure 5.

GRABS scores were correlated with S-scores from the chemical genomics dataset in (Nichols et al., 2011). SDS, sodium dodecyl sulfate.

Condition	Correlation coefficient
Chloropromazine, 12.0 μg/mL	0.092
Calcofluor	0.079
Chloropromazine, 3.0 μg/mL	0.079
Ceftazidime, 0.05 μg/mL	0.078
Cefsulodin, 12.0 μg/mL	0.076
SDS, 3.0%	0.075
Cefsulodin, 6.0 μg/mL	0.075
Cefoxitin, 1.0 μg/mL	0.07
Chloropromazine, 6.0 μg/mL	0.07
Trimethoprim, 0.4 μg/mL	0.068
Dibucaine, 0.8 μg/mL	0.068
Cefaclor, 2.0 μg/mL	0.068
Nigericin, 0.1 μg/mL	0.065
Ampicillin, 8.0 μg/mL	0.065
SDS, 2.0%	0.064
Doxorubicin, 1.0 μg/mL	0.063
Bacitracin, 300 μg/mL	0.063
Ultraviolet light, 18 s	0.061
Cefoxitin, 0.75 μg/mL	0.059
pH 4	0.059

Table S4: Chemical-genomics conditions with the largest-magnitude negative Pearson correlation coefficients with stiffness scores. Related to Figure 5.

GRABS scores were correlated with S-scores from the chemical genomics dataset in (Nichols et al., 2011). MMS, methyl methanesulfonate; CCCP, carbonyl cyanide *m*-chlorophenyl hydrazone.

Condition	Correlation coefficient
Amoxicillin, 0.5 μg/mL	-0.081
Amoxicillin, 0.25 μg/mL	-0.069
Thiolactomycin, 5.0 μg/mL	-0.062
MMS, 0.05%	-0.060
Tetracycline, 1.0 μg/mL	-0.057
Gentamycin, 0.1 μg/mL	-0.056
Tetracycline, 0.75 μg/mL	-0.056
Thiolactomycin, 1.0 μg/mL	-0.053
CCCP, 0.5 μg/mL	-0.053
CHIR-090, 0.02 μg/mL	-0.053
Nitrofurantoin, 0.5 μg/mL	-0.052
Oxacillin, 5.0 μg/mL	-0.051
Theophylline, 100.0 μg/mL	-0.051
Oxacillin, 0.5 μg/mL	-0.050
High nickel, 0.1 μg/mL	-0.050
Norfloxacin, 0.01 μg/mL	-0.049
Nitrofurantoin, 1.0 μg/mL	-0.048
CCCP, 2.0 μg/mL	-0.046
CCCP, 0.1 μg/mL	-0.046
High nickel, 1.0 μg/mL	-0.046

Table S5: Liquid growth-curve data for Keio strains in the absence of kanamycin. Related to Figure 2. Optical density (λ = 595 nm) was measured as a function of time. Growth data are included as a separate text file.

182 **Table S6: Strains and plasmids used in this study. Related to Figures 1–5.**

Strain	Description	Reference/source
MG1655	*E. coli* K-12 wildtype	CGSC #6300
BW25113	*E. coli* (Keio collection parent)	(Baba *et al*., 2006a)
Keio collection	Single deletion mutants (numbered JW####)	(Baba *et al*., 2006a)
DH5α	F−*endA*1 *glnV*44 *thi*-1 *recA*1 *relA*1 *gyrA*96 *deoR nupG* Φ80d*lacZ*ΔM15 Δ(*lacZYA-argF*)U169, *hsdR*17(rK− mK+)	Invitrogen
DH5α(λpir)	F−*endA*1 *glnV*44 *thi*-1 *recA*1 *relA*1 *gyr*A96 *deoR nupG* Φ80d*lacZ*ΔM15 Δ(*lacZYA-argF*)U169, *hsdR*17(rK− mK+) λ::pir	Invitrogen
MFDpir	MG1655, RP4-2-Tc::[ΔMu1::*aac*(3)IV-Δ*aphA* Δ*nic*35 ΔMu2::*zeo*] Δ*dapA*::(*erm*-pir) Δ*recA*	(Ferrieres *et al.*, 2010)
HTC1	MG1655 Δ*mrcB*	This study
HTC2	MG1655 Δ*lpoB*	This study
HTC3	MG1655 Δ*mrcA*	This study
HTC4	MG1655 Δ*lpoA*	This study
HTC5	MG1655 Δ*hscA*	This study
HTC6	MG1655 Δ*hfq*	This study
BW25113-E1	BW25113 pBAD33 c280	This study
JW3359-E1	BW25113 *mrcA* : kan pBAD33c280	This study
JW3116-E1	BW25113 *lpoA* : kan pBAD33c280	This study
JW5157-E1	BW25113 *lpoB* : kan pBAD33c280	This study
JW2510-E1	BW25113 *hscA* : kan pBAD33c280	This study
JW4130-E1	BW25113 *hfq* : kan pBAD33c280	This study
JW3359-C	BW25113 *mrcA* : kan pBAD33c280-*mrcA*	This study
JW3116-C	BW25113 *lpoA* : kan pBAD33c280-lpoA	This study
JW5157-C	BW25113 *lpoB* : kan pBAD33c280-lpoB	This study
JW2510-C	BW25113 *hscA* : kan pBAD33c280-	This study

	hscA	
JW4130-C	BW25113 *hfq* : kan pBAD33c280-*hfq*	This study
BW25113-E2	BW25113 pAM238	This study
JW0145-E2	BW25113 *mrcB* : kan pAM238	This study
JW5157-E2	BW25113 *lpoB* : kan pAM238	This study
JW1045-C	JW0145 psK12	This study
HTC7	JW0145 psK12-R190D	This study
HTC8	JW0145 psK12-D163A/E166A	This study
HTC9	JW0145 psK12-E233Q (∗GT)	This study
HTC10	JW0145 psK12-S510A (∗TP)	This study
HTC11	JW0145 psK12-D163A/E166A/E187A/ N188A/R190A/Q191A (6UB2H)	This study
HTC12	JW0145 psK12-(∗TP/∗GT)	This study
HTC13	JW0145 psK12-(∗6UB2H/∗TP)	This study
HTC14	JW0145 psK12-(∗6UB2H/∗GT)	This study
HTC15	JW0145 psK12-(∗6UB2H/∗TP/∗GT)	This study
BW25113-sulA	BW25113 pDB192	This study
JW3359-sulA	BW25113 *mrcA* : kan pDB192	This study
JW3116-sulA	BW25113 *lpoA* : kan pDB192	This study
JW1045-sulA	BW25113 *mrcB* : kan pDB192	This study
JW5157-sulA	BW25113 *lpoB* : kan pDB192	This study
JW2510-sulA	BW25113 *hscA* : kan pDB192	This study
JW4130-sulA	BW25113 *hfq* : kan pDB192	This study
JW4216-sulA	BW25113 *holC* : kan pDB192	This study
JW2512-sulA	BW25113 *iscA* : kan pDB192	This study
JW2050-sulA	BW25113 *dcd* : kan pDB192	This study
JW1075-sulA	BW25113 *rpmF* : kan pDB192	This study
JW1065-sulA	BW25113 *flgG* : kan pDB192	This study
JW0891-sulA	BW25113 *aro*A : kan pDB192	This study
JW2669-sulA	BW25113 *recA* : kan pDB192	This study
BW25113-E3	BW25113 PUA66	This study
JW1045-E3	BW25113 *mrcB* : frt pUA66	This study
JW5157-E3	BW25113 *lpoB* : frt pUA66	This study
JW2510-E3	BW25113 *hscA* : frt pUA66	This study
JW4130-E3	BW25113 *hfq* : frt pUA66	This study

JW2512-E3	BW25113 *iscA* : frt pUA66	This study
JW2669-E3	BW25113 *recA* : frt pUA66	This study
BW25113-sulA-R	BW25113 PUA66-*sulA*-GFP	This study
JW1045-sulA-R	BW25113 *mrcB* : frt pUA66-*sulA*-GFP	This study
JW5157-sulA-R	BW25113 *lpoB* : frt pUA66-*sulA*-GFP	This study
JW2510-sulA-R	BW25113 *hscA* : frt pUA66-*sulA*-GFP	This study
JW4130-sulA-R	BW25113 *hfq* : frt pUA66-*sulA*-GFP	This study
JW2512-sulA-R	BW25113 *iscA* : frt pUA66-*sulA*-GFP	This study
JW2669-sulA-R	BW25113 *recA* : frt pUA66-*sulA*-GFP	This study
Plasmid	Description	Reference/source
pDS132	R6K ori, *sacB*, MCS, *cat*, CmR	(Phillipe *et al*., 2004)
pBAD33 c280	pACYC ori, pBAD promoter, MCS, *cat*, CmR	(Lee *et al*., 2007)
pAM238	pSC101 ori, pLac, SpecR	(Gonzalez *et al*., 2010)
pSK12	pAM238-*mrcB*	(Ranjit and Young, 2013)
pDB195	*sulA*, pLac, AmpR, CarbR	(Amir *et al*., 2014)
pUA66	gfpmut2, KanR	GE Dharmacon
pUA66-*sulA*-GFP	*sulA* promoter, *sulA-gfpmut2*	GE Dharmacon

183

184 **Table S7. Primers used in this study (5′ to 3′). Related to Figure 4.**

Primer (pBAD33 c280)	Sequence
mrcA_C-Fwd	CATGTCTAGATTACGCCAGACGCGGGTTAA
mrcA_C-Rev	CATGTCTAGAGTGAAGTTCGTAAAGTATTTTT
lpoA_C-Fwd	CATGTCTAGAATGGTACCCTCAACATTTTCTCG
lpoA_C-Rev	CATGTCTAGATTAACTGACGGGGACTACCTGA
lpoB_C-Fwd	CATGTCTAGAATGACAAAAATGAGTCGCTAC GC
lpoB_C-Rev	CATGTCTAGATTATTGCTGCGAAACGGCACCT
hscA_C-Fwd	CATGTCTAGAATGGCCTTATTACAAATTAGTG AACCT
hscA_C-Rev	CATGTCTAGATTAAACCTCGTCCACGGAATG
hfq_C-Fwd	CATGTCTAGAATGGCTAAGGGGCAATCTTTAC A
hfq_C-Rev	CATGTCTAGATTATTCGGTTTCTTCGCTGTCCT
Primer (pSK12)	Sequence
mrcB_R190D_Fwd	CGTCAATATGGAGAACAACGATCAGTTCGGTT TCTTCCG
mrcB_R190D_Rev	CGGAAGAAACCGAACTGATCGTTGTTCTCCAT ATTGACG
mrcB_D163A/E166A_Fwd	CCGTTTGATTTCCCGGCCAGTAAAGCAGGACA GGTGCGCGCG
mrcB_D163A/E166A_Rev	CGCGCGCACCTGTCCTGCTTTACTGGCCGGGA AATCAAACGG
mrcB_R190A/Q191A_Fwd	CGTCAATATGGCGGCCAACGCTGCGTTCGGTT TCTTCCG
mrcB_R190A/Q191A_Rev	CGGAAGAAACCGAACGCAGCGTTGGCCGCCA TATTGACG
mrcB_E187A/N188A_Fwd	CGTCAATATGGCGGCCAACCGTCAGTTCGGTT TCTTCCG
mrcB_E187A/N188A_Rev	CGGAAGAAACCGAACTGACGGTTGGCCGCCA TATTGACG
mrcB_S510A_Fwd	GCGTCGTTCGATTGGTGCCCTTGCAAAACCAG CG
mrcB_S510A_Rev	CGCTGGTTTTGCAAGGGCACCAATCGAACGAC GC
mrcB_E233Q_Fwd	GGATACTTTGCTGGCGACACAAGACCGTCATT TTTACG

mrcB_E233Q_Rev	CGTAAAAATGACGGTCTTGTGTCGCCAGCAAAGTATCC
Primer (pDS132)	Sequence
lpoA_Del_N_term_Fwd	GCATGCAGCGCATCACGGCGGCCT
lpoA_Del_N_term_Rev	TGGTACTCTAGCCATAATGTATCCAGTGATATTTTTTTACGCAATGCTCAATATTAAATCGGC
lpoA_Del_C_term_Fwd	ATCACTGGATACATTATGGCTACAGTACCAACAAG
lpoA_Del_C_term_Rev	ATTGAGCAGAGACTGAAC
lpoB_Del_N_term_Fwd	TTGCCGAAGATGGCTATC
lpoB_Del_N_term_Rev	GCTGCGAAACGGCACCAAGATTCACCCCTTACAAATATAG
lpoB_Del_C_term_Fwd	AAGGGGTGAATCTTGGTGCCGTTTCGCAGCAAT
lpoB_Del_C_term_Rev	CTGACGCGCTATGCACTAAATTTC
mrcA_Del_N_term_Fwd	AGTAAGCAGCGTTGCCAG
mrcA_Del_N_term_Rev	GAAGCGCCT TTTTAATGGAAATTTCCCATTTAGTTTCATTTG
mrcA_Del_C_term_Fwd	AATGGGAAATTTCCATTAAAAAGGCGCTTCGGC
mrcA_Del_C_term_Rev	ATCCTGATCCGCGAATAC
mrcB_Del_N_term_Fwd	AAATCACTCGACATTTATCAGG
mrcB_Del_N_term_Rev	TTTCACGCTTAGATGGCTTTTTCTCCGCAATATTC
mrcB_Del_C_term_Fwd	TTGCGGAGAAAAAGCCATCTAAGCGTGAAATACCG
mrcB_Del_C_term_Rev	TCAGGTGGTCATAGGTGTTG
hscA_Del_N_term_Fwd	ATGGATTACTTCACCCTC
hscA_Del_N_term_Rev	ACAATCTTTGGCATAGTTTAGCTTCCAGAAATTAAAAATC
hscA_Del_C_term_Fwd	TTCTGGAAGCTAAACTATGCCAAAGATTGTTATTTTGCCTCATCAGG
hscA_Del_C_term_Rev	GCCAACGCATCTGCGGCG
hfq_Del_N_term_Fwd	CTTCAGGAGGTAGATCCG
hfq_Del_N_term_Rev	AAACAGCCCGAAACCTCTCTCTTTTCCTTATATGCTTATTTG
hfq_Del_C_term_Fwd	TAAGGAAAAGAGAGAGGTTTCGGGCTGTTTTTTTAC
hfq_Del_C_term_Rev	CATGCGTACGCCTTTCTGTCTTTCAAGGTG

EXTENDED EXPERIMENTAL PROCEDURES

Strain and plasmid construction

Table S6 lists the strains and plasmids used in this study for cloning. Primers are described in Table S7. Screening was performed using the Keio collection of non-essential single-gene deletion mutants (Baba et al., 2006). We used allele exchange to individually delete genes in frame in *E. coli* MG1655 without leaving a scar on the chromosome after excision (Philippe et al., 2004).

Growth of bacterial cultures for screening

Individual 2-mL cultures were inoculated from a freezer stock and grown overnight in lysogeny broth (LB) at 37 °C with shaking until saturation (~16 h). For this initial overnight culture, Keio mutants were grown in the presence of 30 μg/mL kanamycin for selection of the Keio mutant. Strains containing plasmid pBAD33 c280 or plasmid pAM238/pSK12 were grown overnight in 30 μg/mL chloramphenicol or 30 μg/mL spectinomycin, respectively.

Preparation of GRABS 96-well plates

The absorbance values (λ = 600 nm) of 1:10 dilutions in LB of saturated overnight cultures of 48 strains grown in tubes were determined using a spectrophotometer

(Amersham Biosciences, Buckinghamshire, UK). Cells were spun down at 800 x *g* for 10 min, the supernatants were removed, and the pellets were resuspended in 1 mL LB to a final density of 0.32 × optical density (OD). To prepare for agarose encapsulation, 48 microstirrers (V&P Scientific, San Diego, CA, USA) were sterilized with 70% ethanol and placed into individual wells in columns 1-6 of a 96-well microplate (Thermo Scientific Nunc, Waltham, MA, USA). The microplate was covered with a lid and sterilized with ultraviolet light for 20 min. After sterilization, the microplate was placed onto our custom magnetic surface composed of two magnets (BZ0Z02-N52; KJ Magnetics, Pipersville, PA, USA) mounted in plastic casing, and a new sterile microplate was inverted on top. The two plates were turned over and placed onto the magnetic surface to draw the microstirrers into the new sterile plate. Finally, a sterile lid was placed onto the new microplate, which was transferred to a 50 °C hotplate to warm the plate and magnets for at least 20 min prior to the addition of agarose. This warming step ensured that the agarose remained in solution after being added to the plate.

Agarose was prepared as a solution of 1% w/v UltraPure agarose (Invitrogen Corporation, Carlsbad, CA, USA) in 20 mL LB. The solution was heated in a microwave until the agarose dissolved completely and the solution was visually homogeneous. The hot agarose solution was placed in a 65 °C water bath for 30 s

while air bubbles rose to the surface. To prepare the final plate for growth-curve measurements, we maintained the microplate at 50 °C and pipetted 150 μL LB into the wells in columns 7-12 (these wells lacked magnets) and let the LB warm for >20 min. Using a positive displacement pipette (Eppendorf, Hamburg, Germany), we added 150 μL of agarose prepolymer from a 2.5-mL tip into each well that contained a magnetic stirrer. Antibiotics were added as necessary and the cultures were mixed with magnetic stirrers for ~10 s. The microplate was transferred to a second hotplate set to 37 °C and cooled for 15-20 s. We aliquoted 5 μL of each cell suspension using a multichannel pipette into one well with LB and one well with agarose prepolymer to yield an OD ~0.01 and mixed the resulting cultures with magnetic stirrers for ~10 s.

We then took the microplate off the hotplate, removed the microplate lid, and rapidly applied the magnetic lid to extract the stirrers out of the wells. We removed the magnetic lid and quickly popped any bubbles on the surface of the agarose gel with a sterile pipette tip to ensure that the gel surface was smooth to enable accurate absorbance readings. The lid was again placed on the microplate, which was incubated at room temperature for 5 min while the agarose solidified. The lid was removed and the plate was sealed with a transparent polymer film (Excel Scientific, Victorville, CA, USA). To reduce condensation on the film, we

made ~0.25-0.5 cm cuts with a razor blade sterilized with 70% ethanol on opposite sides of each well near its edge. Finally, we placed the microplate into a preheated 37 °C M1000 plate reader (Tecan, Mannedorf, Switzerland) and acquired growth curves at 37 °C by measuring absorbance at 595 nm. The orbital and linear shaking durations were 30 s and 15 s, respectively, and the shaking amplitude was 2 mm. Readings were taken for 16 h at 1-min intervals. The Tecan M1000 plate reader was driven using i-control v. 1.9.17.0 (Tecan), which was used to collect and export data for further analysis.

GRABS measurements in variable agarose concentrations

E. coli BW25113 was inoculated from a freezer stock into 2 mL LB and grown overnight at 37 °C in a shaking incubator. We measured the absorbance (λ = 600 nm) of a 1:10 dilution in LB of the overnight culture and calculated the volume of culture needed for resuspension in 1 mL of fresh medium for a final absorbance of 2. This volume of cells was spun down at 800 x *g* for 10 min, the supernatant was removed, and the pellet was resuspended in 1 mL LB. The cells were stored at 37 °C until use (within 5 min).

A stock solution of 5% (w/v) agarose was prepared by dissolving UltraPure agarose into 65 mL LB and placing the solution in a 70 °C water bath. Twenty-

266 milliliter working solutions of 0.25-5% (w/v) agarose were prepared in 50-mL
267 conical tubes by diluting the appropriate volume of 5% (w/v) agarose in
268 preheated LB. These solutions were also placed into the 70 °C water bath. Using
269 a positive displacement pipette, 2 mL of the agarose working solutions were
270 aliquoted into individual preheated glass test tubes and kept at 65 °C in a water
271 bath. Individual tubes were subsequently removed from the 70 °C water bath
272 and allowed to cool in a 37 °C water bath for ~20 s. Ten microliters of the cell
273 suspension were added to each test tube, yielding a final cell density in solution
274 of 0.01 (λ = 600 nm), and the tube was vigorously shaken to ensure homogenous
275 incorporation of the cells into the agarose solution. Using a positive displacement
276 pipette, 150 μL of the agarose cell solution were pipetted into a 96-well
277 microplate in replicate ($n \geq 3$). This process was repeated for each agarose
278 concentration. We also monitored growth in liquid LB in order to determine the
279 percent inhibition of each gel compared to liquid. The liquid control was
280 prepared at room temperature with the same cell suspension used for the
281 agarose growth curves. The plate was placed on the bench at room temperature
282 for ~3 min in order to allow the agarose wells to solidify. Growth was monitored
283 with a plate reader.
284
285 **GRABS data analysis**

Growth data were collected over 16 h for Keio mutants in both agarose and liquid medium. To reduce the growth curve to a scalar value, we first normalized the growth data in liquid and agarose by subtracting the minimum OD reading (in agarose and liquid) for each mutant. Next, we averaged the 10 min of growth before the 8 h time point, which is approximately when BW25113 cells begin to enter stationary phase in liquid medium (Figure S3A-C). Cells tend to reach saturation at later time points when embedded in agarose (Figure S3A-C), and thus our mechanical phenotype is sensitive to the time point of measurement; t = 8 h was selected because it provided the largest dynamic range of values (Figure S3A-C). We then determined a percent growth value for each mutant compared to wildtype. The GRABS score is a relative percentage of wild-type OD, calculated as $((OD_{mutant,agarose}/OD_{WT,agarose}) - (OD_{mutant,liquid}/OD_{WT,liquid}))$. A positive growth value indicates an increase in GRABS score, and a negative growth score indicates a decrease in GRABS score. Note that this GRABS score is a measure of cell mechanics that is complementary, but not identical, to the Young's modulus. For our screen in kanamycin, we normalized all mutant data to an average of several wild-type growth curves in liquid and agarose. In our secondary screen in LB, we used the wild-type control on each plate to normalize the data.

Analysis of cell morphology

306 To estimate the average cell morphology across the Keio collection, images from
307 the National BioResource Project were segmented with a custom MATLAB
308 software package (Ursell et al., 2014). At least 100 cells were included in the
309 calculation of average cell width and length for each Keio mutant.
310
311 **Correlation with chemical-genomics data**
312 To compare GRABS scores against colony growth data from a variety of chemical
313 conditions, we calculated the Pearson correlation coefficient between the GRABS
314 scores for all tested mutants and the S-scores for the equivalent mutants in the
315 chemical condition from Ref. (Nichols et al., 2011). The significance of the
316 correlation for each condition was estimated by comparing the correlation score
317 against the correlation of 1000 random permutations of S-scores.
318
319 **Complementation and deletion assays for GRABS hits and PBP1b mutants**
320 Keio-complementation and wild-type control strains were streaked out from
321 freezer stock onto LB agar plates with appropriate antibiotics to obtain
322 individual colonies. Individual colonies were inoculated into 2 mL LB with
323 appropriate antibiotics and grown overnight at 37 °C. Saturated overnight
324 cultures were diluted 1:100 into 2 mL fresh LB (without antibiotics) and grown to
325 an absorbance of ~0.6 (λ = 600 nm). Microplates were prepared as described

above. For complementation assays, antibiotics were not added to microplate wells so as to not influence the growth of the cells. Five microliters of a 2.5 mM arabinose stock solution were added to the wells containing strains with plasmid pBAD33 c280; the final arabinose gel concentration was 0.08 mM. Strains with wildtype or mutant PBP1b under the control of isopropyl β-D-1-thiogalactopyranoside were not induced; the basal level of expression from the *lac* operon was sufficient for full complementation of the stiffness defect (Figure S4A). Growth curves were compared to curves for the appropriate empty vector/native PBP1b controls to confirm recovery or loss of cell stiffness when the proteins were expressed in *trans*.

E. coli MG1655 mutants (Δ*mrcB*, Δ*mrcA*, Δ*lpoB*, Δ*lpoA*, Δ*hscA*, and Δ*hfq*) were streaked out from freezer stocks onto LB agar plates to obtain individual colonies. Individual colonies were inoculated into 2 mL LB and grown overnight at 37 °C. Wild-type and mutant strains were screened for stiffness changes as described above and compared to the corresponding BW25113 mutants.

Confirmation of chemical effectors of GRABS measurements

E. coli BW25113 and 45 additional Keio strains were grown overnight from freezer stock until saturation, in the appropriate antibiotic. Carbonyl cyanide *m*-

chlorophenyl hydrazone (CCCP, Sigma-Aldrich) stock was prepared by dissolving CCCP into dimethyl sulfoxide (DMSO) (Sigma-Aldrich, St. Louis, MO, USA). CCCP was diluted into 1 mL LB to yield a 64 μg/mL working solution. The GRABS plate and cells were prepared as described above. During preparation of the GRABS plate, 5 μL CCCP were added to each well. The final concentrations of CCCP and DMSO in the plate were 2 μg/mL and ~0.1%, respectively. Appropriate DMSO-only controls were performed to confirm that DMSO did not affect the GRABS score. The percent growth values were determined as described, using the BW25113 (DMSO+) and (CCCP+) wells to normalize data from the mutants.

Microscopy-based stiffness measurements

Single-cell measurements of encapsulated cell growth were performed in 1-4% (w/v) agarose as described previously (Tuson et al., 2012). Briefly, bacteria were grown in liquid LB without antibiotics to an absorbance (λ = ◎◎◎ ◎◎) of ~0.6. Cells were diluted 1:100 and spotted onto 2% agarose pads. Elongation was monitored on a Nikon Eclipse Ti inverted microscope (Nikon, Tokyo, Japan) equipped with a heated stage (Okolab, Pozzuoli, Italy) and objective heater (Bioptechs, Butler, PA, USA) at 37 °C. Images were collected over a 30-min period at 1-min intervals using a CoolSNAP HQ2 camera (Photometrics, Munich, Germany). Cell length

366 was measured for each mutant and wild-type strain using MicrobeTracker
367 (Sliusarenko et al., 2011). Length measurements were halted after cells divided.
368 We calculated the fractional elongation over time for each mutant, averaged over
369 all single cells (Tuson et al., 2012).
370
371 **Microfluidic-based stiffness measurements**
372 Keio mutants and wild-type strains were transformed with a plasmid (pDB192)
373 containing *sulA* under an isopropyl β-D-1-thiogalactopyranoside-inducible
374 promoter. The strains were grown overnight in 2 mL LB containing 30 μg/mL
375 kanamycin and 50 μg/mL ampicillin. We fabricated and applied a microfluidic
376 device to the determination of cellular bending rigidity and Young's modulus as
377 described previously (Amir et al., 2014). As an alternative means of causing cells
378 to filament, we applied 1 μg/mL aztreonam (MP Biomedicals, CA, USA).
379 Deflection of cells under fluid flow was monitored on a Zeiss Axiovert 100
380 microscope (Zeiss, Oberkochen, Germany) equipped with a 60X oil objective.
381 Images were collected with an Andor iXon 3 EMCCD (Andor, Belfast, UK) using
382 μManager v. 1.4.16 (Edelstein et al., 2010). Deflection of the cells was determined
383 using a custom Igor Pro (WaveMetrics Inc.) image analysis algorithm.
384

To account for changes in the diameter of mutant cells compared to wild-type cells after filamentation, we collected static images on a Nikon Eclipse Ti inverted microscope equipped with a 60X oil objective (Nikon) using a CoolSNAP HQ2 camera (Photometrics). Cell width was measured using MicrobeTracker (Sliusarenko et al., 2011). These measurements were used to calculate the Young's modulus from the flexural rigidity, in which the moment of inertia (I) of a cross-section is dependent on cell radius (r) and thickness of the cell wall (h) according to $I = \pi r^3 h$.

Cell death in 1% agarose and liquid

The GRABS assay for Keio mutants and wild-type strains was carried out as described above. One hundred and fifty microliters of liquid LB and agarose (prior to gelling) were pipetted out of the 96-well plate and transferred to an 8-well LAB-TEK II chambered coverglass #1.5 (Nunc, NY, USA). The agarose was allowed to solidify at room temperature. LAB-TEK II chambers were placed into a 37 °C incubator with shaking for 8 h, at which point the GRABS score was determined. After 8 h, cells were removed from the 37 °C incubator and labeled via the LIVE/DEAD BacLight Viability Kit (L7007, Invitrogen) at room temperature. For staining of cells grown in liquid, cells were diluted 1:20 in fresh LB and stained in the dark for 20 min according to the manufacturer's guidelines.

For staining of cells grown in agarose, 25 μL of a stock solution (100 μL component A (1.67 mM SYTO 9, 1.67 mM Propidium iodide) + 1.5 μL component B (1.67 mM SYTO 9, 18.3 mM Propidium iodide)) were pipetted onto the agarose surface and allowed to diffused through the gel in the dark for 30 min. Cells were imaged with epifluoresence using a Nikon Ti inverted microscope equipped with a CoolSNAP HQ2 camera (Photometrics) and a 100X oil objective (Nikon).

Purification of sacculi and ultra performance liquid chromatography (UPLC) of peptidoglycan composition

Overnight cultures of *E. coli* BW25113 or Keio strains were diluted 1:100 in LB and grown at 37 °C to an OD_{600} of 0.7. The cultures were then harvested by centrifugation at 5,000 × *g* for 10 min at room temperature and resuspended in 3 mL LB. Cell suspensions were lysed by boiling in sodium dodecyl sulfate, and insoluble material was collected by several rounds of ultracentrifugation at 400,000 × *g* for 20 min at room temperature. Samples were prepared for UPLC as previously described (Brown et al., 2012) and injected onto a Waters H Class UPLC system equipped with a BEH C18 1.7-μm column (Waters, MA, USA), using elution conditions previously described (Desmarais et al., 2014). Peaks were quantified and identified as particular muropeptide species using the

software package Chromanalysis (Desmarais et al., 2015), from which the crosslinking density and strand length were calculated (Ottolenghi et al., 1993; Pisabarro et al., 1985).

Shape of agarose-embedded cells

The GRABS assay for Keio mutants and wild-type strains was carried out as previously described. One hundred and fifty milliliters of agarose (prior to gelling) were pipetted out of the 96-well plate and transferred to an 8-well LAB-TEK II chambered coverglass #1.5 w/cover (Nunc, NY, USA). The agarose was allowed to solidify at room temperature. LAB-TEK II chambers were placed into a 37 °C incubator with shaking for 8 h (at which point the GRABS score is typically determined). After 8 h, cells were removed from the incubator and labeled with FM 4-64 FX (Invitrogen). For staining, 25⊚μL of a 100 ⊚g⊚⊚L stock were pipetted onto the surface of the agarose and allowed to diffuse through the gel, in the dark, for 30 min. Cells were imaged using phase contrast and epifluoresence microscopy.

Cell density versus OD measured by plate reader

A saturated overnight culture of *E. coli* BW25113 was diluted 1:100 into 60 mL of fresh LB and grown in a 37 °C incubator with shaking until an absorbance of 3.0

(λ = 600 nm). We calculated the volume of the culture needed for resuspension in 200 μL of fresh LB medium for a final absorbance of 248 OD. This volume of cells was spun down at 800 × *g* for 10 min, the supernatant was removed, and the pellet was resuspended in fresh LB media. A 2-fold dilution series was made from 240 OD to 0.007 OD. Five microliters of diluted culture were inoculated into agarose for a final cell density in the plate of 8 OD-0.0004 OD. The OD (λ = 595 nm) was measured immediately using a Tecan M200 PRO plate reader.

Measurement of SOS using a promoter-fusion assay

To measure SOS induction we used the plasmids pUA66-*sulA* promoter-GFP (p*SulA*-GFP) and the empty vector control pUA66-GFP (pUA66) transformed in the Keio parent strain *E.coli* BW25113 and the Keio strains (Δ*mrcB*, Δ*lpoB*, Δ*hscA*, Δ*hfq*, Δ*iscA*, Δ*recA*). Three biological replicates of wildtype cells and Keio strains containing p*SulA*-GFP and pUA66 were inoculated from a plate of overnight cultures in LB and grown at 37 °C in an incubator with shaking. The GRABS assay was carried out as described above. As a positive control to test the effects of inducing the SOS response, norfloxacin was added at three times the minimum inhibitory concentration (30 ng/mL) to wild-type cells grown in liquid and embedded in agarose. OD was measured at λ = 595 nm and GFP

fluorescence was measured with excitation at 485 nm and emission at 515 nm using a Tecan M200 PRO plate reader at 10 min intervals for 8 h.

Analysis of SOS induction was performed by first normalizing the data to fluorescence intensity per cell for p*SulA*-GFP and pUA66 at each time point (t) using the ratio (fluorescence intensity(t)/optical density(t)). We corrected for basal GFP expression by subtracting normalized fluorescence values of pUA66 from p*sulA*-GFP at each time point: (p*SulA*-GFP$_{\text{normalized}}(t)$ – pUA66$_{\text{normalized}}(t)$). 3 biological replicates were averaged at each time point. We subtracted average fluorescence values at $t = 0$ from each subsequent time point to monitor changes in SOS induction for 1% agarose and liquid.

Supplemental References

Amir, A., Babaeipour, F., McIntosh, D.B., Nelson, D.R., and Jun, S. (2014). Bending forces plastically deform growing bacterial cell walls. Proceedings of the National Academy of Sciences of the United States of America *111*, 5778-5783.

Baba, T., Ara, T., Hasegawa, M., Takai, Y., Okumura, Y., Baba, M., Datsenko, K.A., Tomita, M., Wanner, B.L., and Mori, H. (2006). Construction of Escherichia coli K-12 in-frame, single-gene knockout mutants: the Keio collection. Mol Syst Biol *2*, 2006 0008.

Brown, P.J., de Pedro, M.A., Kysela, D.T., Van der Henst, C., Kim, J., De Bolle, X., Fuqua, C., and Brun, Y.V. (2012). Polar growth in the Alphaproteobacterial order Rhizobiales. Proc Natl Acad Sci USA *109*, 1697-1701.

Desmarais, S.M., Cava, F., de Pedro, M.A., and Huang, K.C. (2014). Isolation and preparation of bacterial cell walls for compositional analysis by ultra performance liquid chromatography. J Vis Exp, e51183.

Desmarais, S.M., Tropini, C., Miguel, A., Cava, F., Monds, R.D., de Pedro, M.A., and Huang, K.C. (2015). High-throughput, Highly Sensitive Analyses of Bacterial Morphogenesis Using Ultra Performance Liquid Chromatography. The Journal of biological chemistry *290*, 31090-31100.

494 Edelstein, A., Amodaj, N., Hoover, K., Vale, R., and Stuurman, N. (2010).
495 Computer control of microscopes using microManager. Current protocols in
496 molecular biology / edited by Frederick M Ausubel [et al] *Chapter 14*, Unit14 20.

497 Nichols, R.J., Sen, S., Choo, Y.J., Beltrao, P., Zietek, M., Chaba, R., Lee, S.,
498 Kazmierczak, K.M., Lee, K.J., Wong, A., *et al.* (2011). Phenotypic landscape of a
499 bacterial cell. Cell *144*, 143-156.

500 Ottolenghi, A.C., Caparros, M., and de Pedro, M.A. (1993). Peptidoglycan
501 tripeptide content and cross-linking are altered in Enterobacter cloacae induced
502 to produce AmpC beta-lactamase by glycine and D-amino acids. J Bacteriol *175*,
503 1537-1542.

504 Philippe, N., Alcaraz, J.P., Coursange, E., Geiselmann, J., and Schneider, D.
505 (2004). Improvement of pCVD442, a suicide plasmid for gene allele exchange in
506 bacteria. Plasmid *51*, 246-255.

507 Pisabarro, A.G., de Pedro, M.A., and Vazquez, D. (1985). Structural modifications
508 in the peptidoglycan of Escherichia coli associated with changes in the state of
509 growth of the culture. J Bacteriol *161*, 238-242.

Sliusarenko, O., Heinritz, J., Emonet, T., and Jacobs-Wagner, C. (2011). High-throughput, subpixel precision analysis of bacterial morphogenesis and intracellular spatio-temporal dynamics. Mol Microbiol *80*, 612-627.

Tuson, H.H., Auer, G.K., Renner, L.D., Hasebe, M., Tropini, C., Salick, M., Crone, W.C., Gopinathan, A., Huang, K.C., and Weibel, D.B. (2012). Measuring the stiffness of bacterial cells from growth rates in hydrogels of tunable elasticity. Mol Microbiol *84*, 874-891.

Ursell, T.S., Nguyen, J., Monds, R.D., Colavin, A., Billings, G., Ouzounov, N., Gitai, Z., Shaevitz, J.W., and Huang, K.C. (2014). Rod-like bacterial shape is maintained by feedback between cell curvature and cytoskeletal localization. Proceedings of the National Academy of Sciences of the United States of America *111*, E1025-1034.